The effect of the distance between acidic site and basic site immobilized on mesoporous solid on the activity in catalyzing aldol condensation

Xiaofang Yu [a], Xiaobo Yu [b], Shujie Wu [a], Bo Liu [a], Heng Liu [a], Jingqi Guan [a,*], Qiubin Kan [a,*]

[a] College of Chemistry, Jilin University, Jiefang Road 2519, Changchun 130023, PR China
[b] China Pharmaceutical University, Nanjing 210009, PR China

ABSTRACT

Acid–base bifunctional heterogeneous catalysts containing carboxylic and amine groups, which were immobilized at defined distance from one another on the mesoporous solid were synthesized by immobilizing lysine onto carboxyl-SBA-15. The obtained materials were characterized by X-ray diffraction (XRD), N_2 adsorption, Fourier-transform infrared spectroscopy (FTIR), thermogravimetric analysis (TGA), scanning electron micrographs (SEM), transmission electron micrographs (TEM), elemental analysis, and back titration. Proximal-C-A-SBA-15 with a proximal acid–base distance was more active than maximum-C-A-SBA-15 with a maximum acid–base distance in aldol condensation reaction between acetone and various aldehydes. It appears that the distance between acidic site and basic site immobilized on mesoporous solid should be an essential factor for catalysis optimization.

Crown Copyright © 2010 Published by Elsevier Inc. All rights reserved.

1. Introduction

Surface-modified mesoporous materials with various active sites have been extensively investigated in recent years for catalysis [1–4], chemical sensing [5], separation [6,7], and nanoscience [8,9]. Many monofunctionalized mesoporous silica catalysts have been demonstrated to have unique properties [10–15]. However, as for many applications, bifunctional or multi-functional mesoporous silica catalysts are much more desirable [16–25], since the combined functionalities may act in a coopera-tive way to improve the reactivity of the catalysts. Much attention has been paid to the combination of organic functional groups, bifunctionalized mesoporous silica nanosphere materials with ureidopropyl group and 3-[2-(2-aminoethylamino)ethylamino]-propyl group [24], or with amine groups and thiols [25]. Zeidan et al. have reported a cooperative effect of SBA-15 containing sulfonic acid and thiol, which exhibits a cooperative effect in a condensation reaction [19]. Dufaud and Davis have reported multifunctional heterogeneous SBA-15 containing primary amine and different acid centers (benzenesulfonic acid, phosphoric acid, or carboxylic acid) [20,21].

Interest in bifunctional catalysts synthesized by controlling spatial arrangement of the functional groups has been growing recently. Site isolation is an effective method to control the distance between functional groups. Our group has reported two acid–base bifunctional mesoporous materials Benzyl-APS-S-SBA-15 and Anthracyl-APS-S-SBA-15 by controlling steric hindrance [26]. Alauzun et al. [27] and Lu et al. [28] have also reported on bifunctionalized mesoporous materials containing an acidic site and a basic site isolated from one another. In addition, bifunctional groups in pairs may be beneficial to achieve cooperative effect. Davis et al. have synthesized acid/thiol paired catalysts involving the design of an organosilane precursor [29,30]. Also, Katz and Bass developed a method to synthesize the thiol/amine paired catalysts based on a xanthate protection strategy to control thiol/amine distance [31].

As reported previously, acid–base cooperative catalysis has been involved in various reactions such as Michael addition [16], aldol condensation [20–22], Henry condensation [16], and Knoevenagel condensation [16,32,33]. The reactions may be focusing on the cooperative action of acid–base groups by the simultaneous activa-tion of both electrophilic and nucleophilic reaction partners. In addition, the amino acids themselves contain carboxylic and amine groups, and they have been used as catalysts in condensation reaction. For example, proline and its derivatives have been proven to be the superior catalysts in the aldol condensation reaction [34–36]. Córdova et al. have also reported that linear amino acids and their derivatives act as catalysts for aldol condensation reaction [37]. However, no report of the linear amino acids that are anchored on solid to perform acid–base cooperative catalysis has appeared.

In this paper, we made an attempt to immobilize different amine group of lysine on mesoporous silica for the synthesis of carboxyl/amine paired catalysts. The carboxylic/amine distance was defined onto the backbones of the mesoporous silica. More-over, how the distance between active sites effected the catalytic activity was explored based on these newly developed materials.

* Corresponding authors. Fax: +86 431 88499140.
E-mail addresses: guanjq@jlu.edu.cn (J. Guan),
catalysischina@yahoo.com.cn (Q. Kan).

2. Material and methods

2.1. Materials

Pluronic123 (Aldrich), HCl (A.R), 4-nitrobenzaldehyde (Acros), 4-(trifluoromethyl)benzaldehyde (Acros), 4-cyanobenzaldehyde (Acros), acetone (A.R), tetraethyorthosilicate (TEOS) (Aldrich), 2-Cyanoethyltriethoxysilane (CTES) (Gelest), H_2SO_4 (A.R), triethylamine (A.R), dimethyl sulfoxide (DMSO) (A.R), and boc-lys-OMe · HCl (Aladdin), H-lys (boc)-OMe · HCl (Aladdin), N-ethyl-N-(3-dimethyl-aminopropyl)carbodiimide hydrochloride (EDC) (Aladdin), and N-hydroxysuccinimide (NHS) (Aladdin) were commercially available and used as received.

2.2. Methods

2.2.1. Preparation of carboxyl-SBA-15 (SBA-15-COOH)

The carboxyl-SBA-15 sample was prepared according to literature procedure [14,15]. In a typical synthesis, 2-cyanopropyl-triethoxysilane (CTES) was introduced to a hydrochloric acid solution of the triblock copolymer Pluronic P123 ($EO_{20}PO_{70}EO_{20}$). After hydrolyzed for 50 min under stirring at 40 °C, tetraethoxysilane (TEOS) was added into the mixture slowly. The molar composition of the mixture was $(1-x)$ TEOS:x CTES:0.017 P123:5.9 HCl:193 H_2O, where $x=0.075$. Next, the resultant mixture was stirred at 40 °C for 20 h, followed by aging at 100 °C for 24 h under static condition. The solid product was recovered by filtration and dried at 60 °C. For removal of the template and hydrolysis of the –CN groups, the dried product was treated with 48.0% H_2SO_4 solution at 95 °C for 24 h. Subsequently, the product was recovered

by washing with water until the eluent became neutral, and finally dried at 90 °C to obtain SBA-15-COOH.

2.2.2. Preparation of Pro-proximal-C-A-SBA-15

Pro-proximal-C-A-SBA-15 was prepared by activating carboxyl-SBA-15 with N-hydroxysuccinimide (NHS), using 1-ethyl-3-(3-dimethylaminopropyl) carbodiimide (EDC) as coupling agent. The 0.5 g boc-lys-OMe · HCl (Excess) was dispersed in 10 ml deionized water, and aqueous 0.19 g NHS and 0.31 g EDC were mixed with 1.2 g SBA-15-COOH/dimethyl sulfoxide (DMSO) solution [38]. Finally, the two solutions were mixed and the pH was adjusted to 8 using triethylamine. The mixture was stirred vigorously at 38 °C for 8 h, and then centrifuged and washed several times with ethanol and copious amount of water. The prepared material with protected groups and proximal carboxylic/amine distance was termed Pro-proximal-C-A-SBA-15 (Scheme 1).

2.2.3. Preparation of Pro-maximum-C-A-SBA-15

Pro-maximum-C-A-SBA-15 with protected groups and enlarged carboxylic/amine distance was synthesized in a similar manner to Pro-proximal-C-A-SBA-15, except that H-lys (boc)-OMe · HCl was used instead of boc-lys-OMe · HCl (Scheme 1).

2.2.4. Preparation of proximal-C-A-SBA-15 and maximum-C-A-SBA-15

After drying the materials of Pro-proximal-C-A-SBA-15 and Pro-maximum-C-A-SBA-15, we deprotected the side chains by shaking in 94% trifluoroacetic solution (water 5% (v/v), triisopropylsilane 1% (v/v)) for 3 h [39]. The solids were collected by filtration with plenty of water and ethanol to give the samples termed proximal-C-A-SBA-15 and maximum-C-A-SBA-15, respectively (Scheme 1).
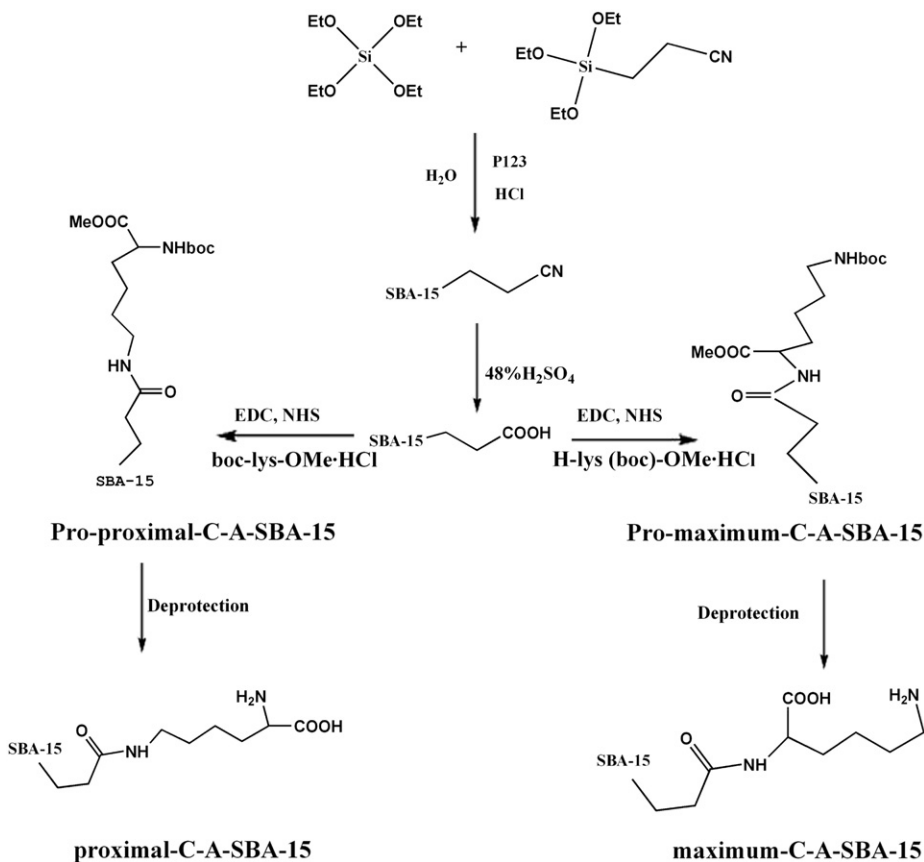
Scheme 1. Synthesis of proximal-C-A-SBA-15 and maximum-C-A-SBA-15.

2.3. Catalytic experiment

The aldol condensation reaction was performed in a flask under nitrogen [20,21]. First, 4-nitrobenzaldehyde (0.76 mg, 0.5 mmol) was dissolved in acetone (10 ml). Each catalytic reaction was carried out over 0.1 g catalyst at 50 °C. After the reaction, the product was filtered with acetone and chloroform to remove the solid catalyst. The resulting product was obtained and analyzed by ^{1}H NMR in CDCl$_3$.

3. Results and discussion

3.1. Characterization

Powder X-ray diffraction patterns (XRD) were collected using a Rigaku D/max-2200 (0.2°/min) with CuKα radiation (40 kV, 40 mA). N$_2$ adsorption–desorption isotherms were obtained on a Micromeritics ASAP 2020 system at liquid N$_2$ temperature (−196 °C). Before measurements, the samples were outgassed at 100 °C for 24 h. The specific surface areas were calculated by using the Brunauer–Emmett–Teller (BET) method and the pore size distributions were measured by using Barrett–Joyner–Halenda (BJH) analysis from the desorption branches of nitrogen isotherms. Therrmogravimetric (TG) analysis was carried out on a Shimadzu DTA-60 working in a N$_2$ stream with a heating rate of 20 °C/min. Transmission electron microscope (TEM) was performed on a Hitachi H-8100 electron microscope, operating at 200 kV. The infrared spectra (IR) of samples were recorded in KBr disks using a NICOLET impact 410 spectrometer. The SEM photographs were taken on a FESEM XL-30 field emission scanning electron microscope. Elemental analyses (EA) were performed on a VarioEL CHN elemental analyzer. A back titration method was used to measure the loading of the carboxyl of the materials according to the modified procedure in literature [26,27]. About 50 mg of the sample was added to a conical beaker, and then 10 ml 0.01 M NaOH solution was added. The mixture was stirred at room temperature for half an hour; then, the mixture was filtered and rinsed repeatedly for four times with 25 ml distilled water. The resulting filtrate was titrated with 0.01 M HCl solution using phenolphthalein as indicator.

Fig. 1 shows the XRD patterns of the samples. All of the XRD patterns showed three well-resolved peaks, indexed as (100), (110),
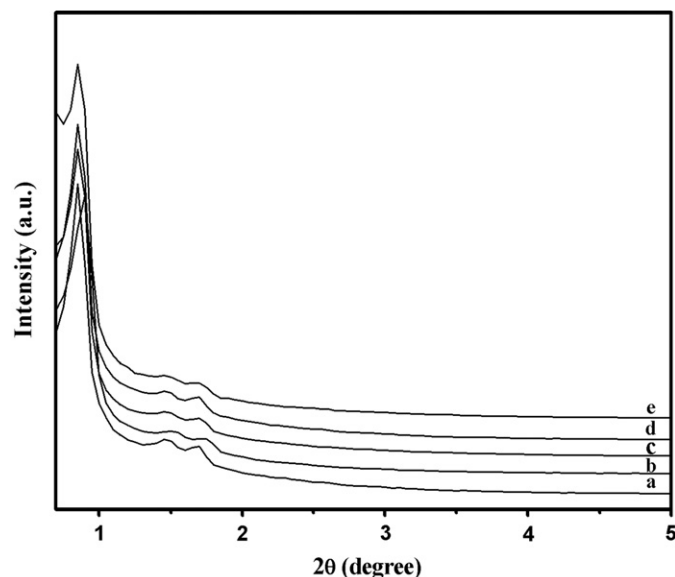
and (200). It indicates that immobilization of lysine onto carboxyl-SBA-15 did not destroy the well-ordered mesoporous structure.

Fig. 2 shows N$_2$ adsorption–desorption isotherms and pore size distributions of the samples. It was found that the samples display a type IV isotherm with H1 hysteresis and a sharp increase in volume adsorbed at $P/P_0 = 0.64$. This indicates that the ordered mesoporous structure was well maintained.

According to the BET analysis in Table 1, proximal-C-A-SBA-15 (588.6 m^2 g^{-1}) and maximum-C-A-SBA-15 (594.2 m^2 g^{-1}) had a significant decrease of BET specific surface areas in comparison with carboxyl-SBA-15 (672.2 m^2 g^{-1}). The obvious reduction in specific surface area and pore volume suggests a successful incorporation of the lysine. However, proximal-C-A-SBA-15 and maximum-C-A-SBA-15 had a significant increase of BET specific surface areas and the pore size in comparison with Pro-proximal-C-A-SBA-15 and Pro-maximum-C-A-SBA-15, which indicates the successful removal of the boc and methyl from Pro-proximal-C-A-SBA-15 and Pro-maximum-C-A-SBA-15.

Fig. 3 shows TEM and SEM images of proximal-C-A-SBA-15 and maximum-C-A-SBA-15, which showed a perfect hexagonal pore structure and a rod-like morphology of carboxyl-SBA-15.

The successful incorporation of the lysine to carboxyl-SBA-15 can be supported by the FT-IR spectra. The IR spectra for synthetic
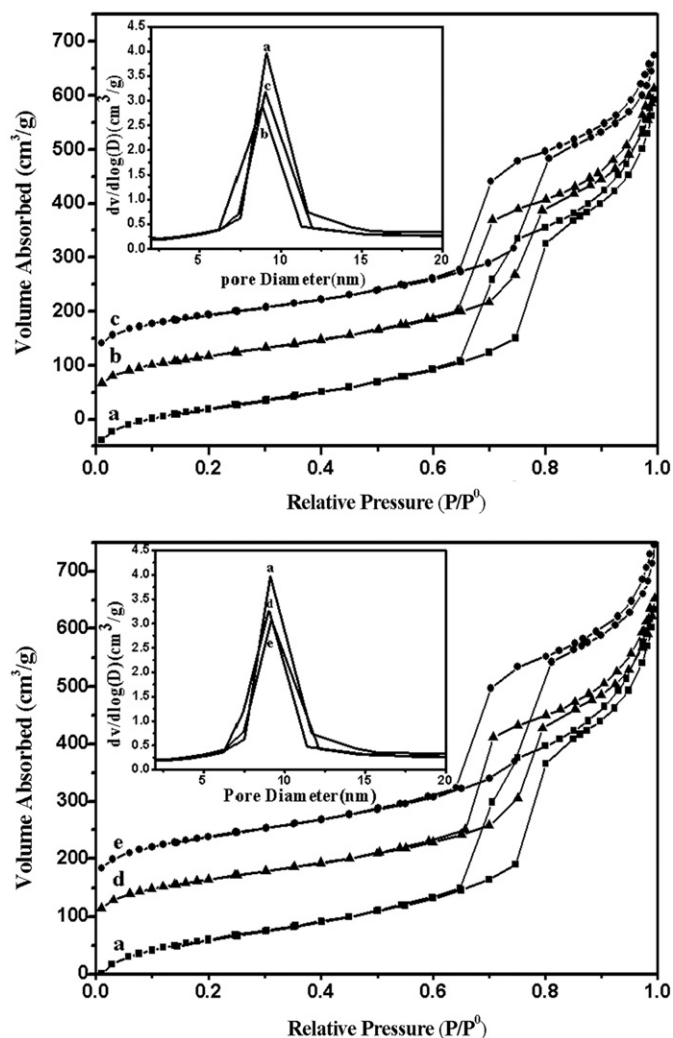
Fig. 2. N$_2$ adsorption isotherm of samples: (a) carboxyl-SBA-15, (b) Pro-proximal-C-A-SBA-15, (c) proximal-C-A-SBA-15, (d) Pro- maximum-C-A-SBA-15, and (e) maximum-C-A-SBA-15.

Fig. 1. XRD diffraction patterns of samples: (a) carboxyl-SBA-15, (b) Pro-proximal-C-A-SBA-15, (c) Pro-maximum-C-A-SBA-15, (d) proximal-C-A-SBA-15, and (e) maximum-C-A-SBA-15.

Table 1
The textural properties of the prepared materials.

Sample	S_{BET} (m² g⁻¹)	D_p (nm)[a]	V_p (cm⁻³ g⁻¹)	N content (w/w%)[b]	Loading of carboxyl (mmol/g)[c]
Carboxyl-SBA-15	672.2	9.09	1.1	–	0.622
Pro-proximal-C-A-SBA-15	557.6	8.93	0.92	–	0.009
Pro-maximum-C-A-SBA-15	556.6	9.01	0.91	–	0.009
Proximal-C-A-SBA-15	588.6	9.02	0.94	0.837	0.613
Maximum-C-A-SBA-15	594.2	9.14	0.95	0.840	0.615

[a] Calculated from desorption branch using the BJH method.
[b] Obtained from CHN elemental analysis.
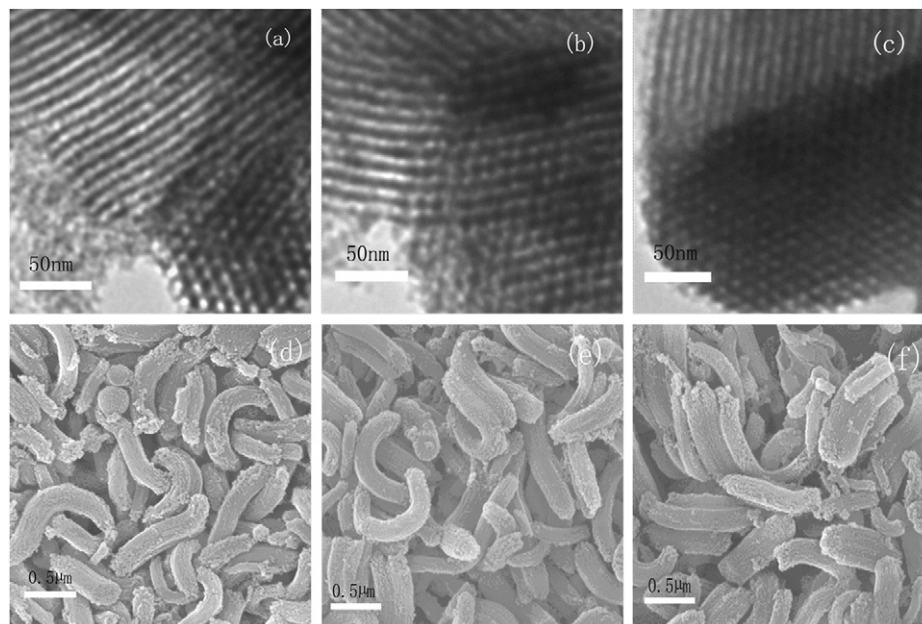[c] Obtained from back titration method.

Fig. 3. TEM and SEM images of samples: (a, d) carboxyl-SBA-15, (b, e) proximal-C-A-SBA-15, and (c, f) maximum-C-A-SBA-15.

samples are shown in Fig. 4. In all the materials, the typical Si–O–Si bands around 1080, 950, and 802 cm⁻¹ associated with the formation of a condensed silica network are present. The strong peaks at 1630 cm⁻¹ could be attributed to H_2O adsorbed in mesopores. The peak at 1718 cm⁻¹ in the spectrum of carboxyl-SBA-15 (Fig. 4a) was attributed to the stretching vibration of C=O in COOH group. However, this peak disappears in Fig. 4b and c, indicating that almost all carboxyl groups were reacted with amino groups of lysine. The peak at 1718 cm⁻¹ was observed after deprotection (Fig. 4d and e), implying that the deprotected step to obtain carboxyl groups is successful. Furthermore, no vibration of the original –CN groups introduced by CTES could be found at 2253 cm⁻¹ in Fig. 4a, proving that all of the –CN groups have been hydrolyzed into -COOH groups through H_2SO_4 treatment. Compared with carboxyl-SBA-15, new peaks at 1560 cm⁻¹ were due to the formation of amide groups (the bending vibration of –NH– groups), further proving that lysine have been incorporated into the backbones of the mesoporous silica. The stretching vibration of –NH– groups at 3383 cm⁻¹ was not resolved due to its overlap with the IR absorptions of silanol groups or hydrogen-bonded water molecule.

Fig. 5 shows the TG profiles of synthetic samples. Weight loss below 100 °C is due to the physically adsorbed water and ethanol inside the pores. The 3–4% weight loss at 100–200 °C is
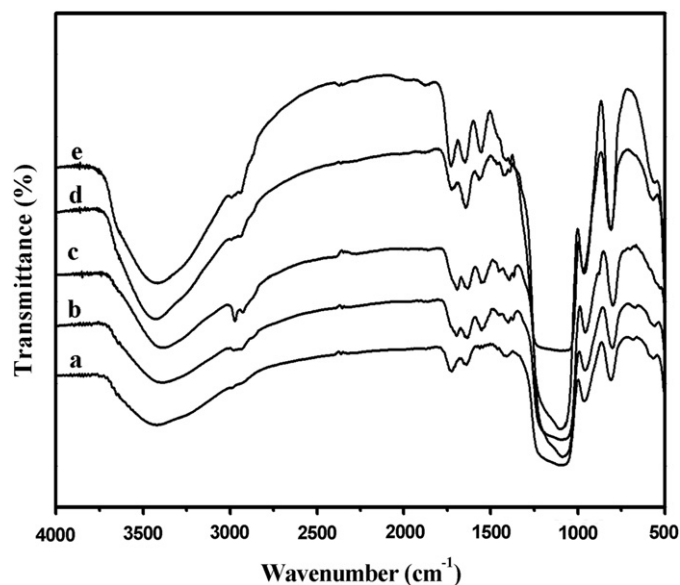

Fig. 4. FTIR spectra of samples: (a) carboxyl-SBA-15, (b) Pro-proximal-C-A-SBA-15, (c) Pro-maximum-C-A-SBA-15, (d) proximal-C-A-SBA-15, and (e) maximum-C-A-SBA-15.
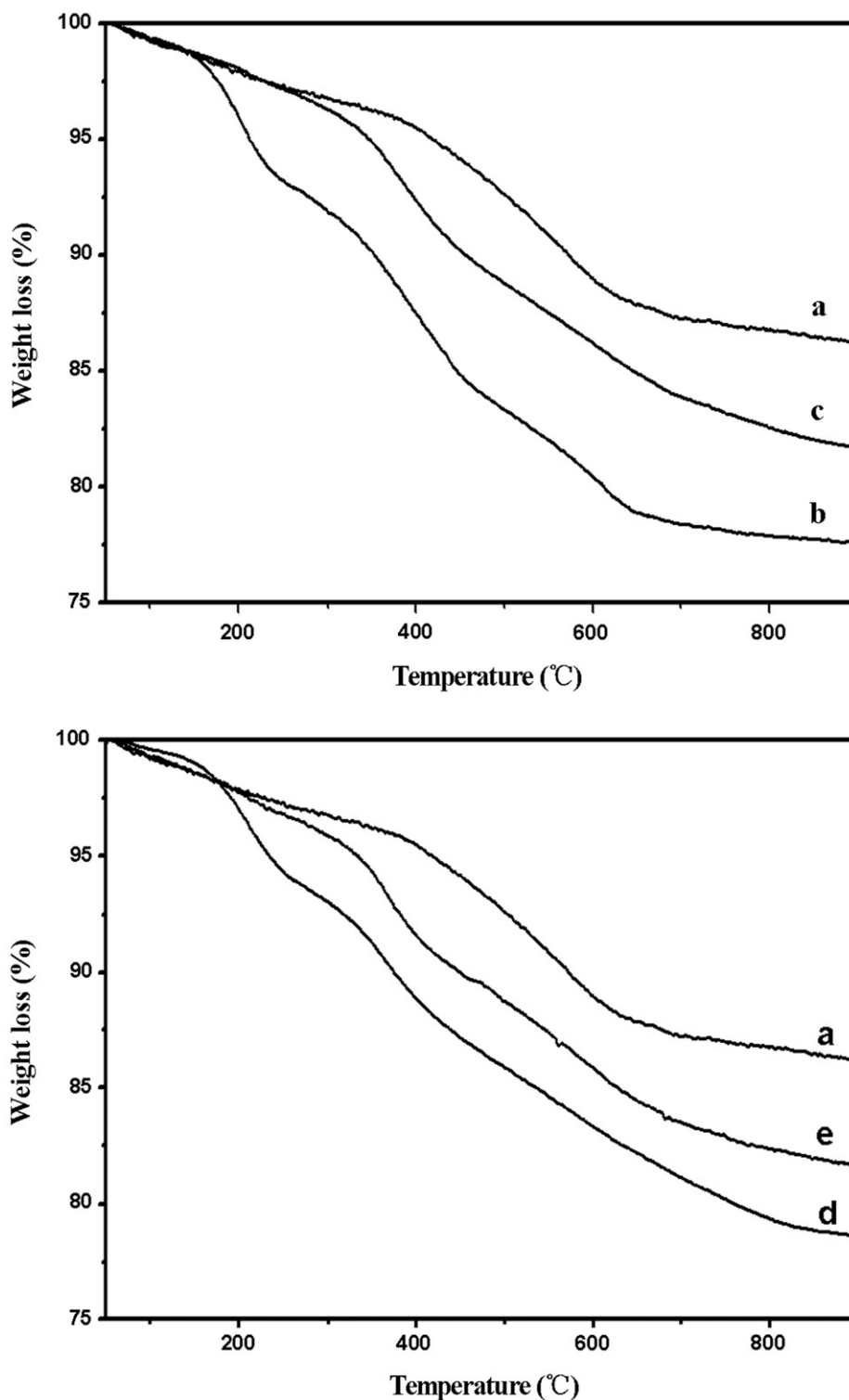
Fig. 5. TG profiles of samples. (a) carboxyl-SBA-15, (b) Pro-proximal-C-A-SBA-15, (c) proximal-C-A-SBA-15, (d) Pro-maximum-C-A-SBA-15, and (e) maximum-C-A-SBA-15.

mainly related to the decomposition of surfactant template. Large weight loss of 3–17% in the temperature range from 200 to 650 °C in proximal-C-A-SBA-15 and maximum-C-A-SBA-15 is probably attributed to the decomposition of organic groups from lysine and a small amount of surfactant template. Comparison with proximal-C-A-SBA-15 and maximum-C-A-SBA-15, excess weight loss in Pro-proximal-C-A-SBA-15 and Pro-maximum-C-A-SBA-15 is probably attributed to the decomposition of protective groups.
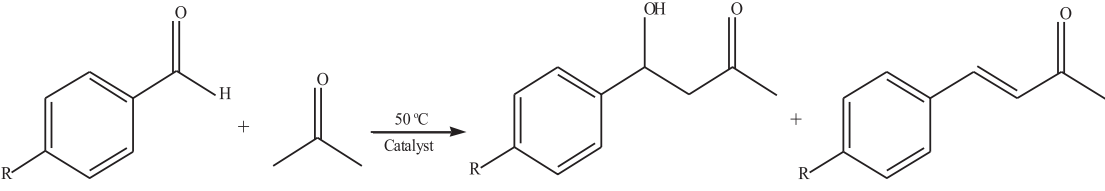
Quantification of the lysine immobilized on SBA-15 was performed using CHN elemental analysis. The results of CHN elemental analysis in Table 1 indicate that there was 0.837% (w/w) of nitrogen for proximal-C-A-SBA-15, 0.840% (w/w) of nitrogen for maximum-C-A-SBA-15. The similar content of nitrogen indicates that proximal-C-A-SBA-15 and maximum-C-A-SBA-15 contained almost the same amount of the lysine.

To further confirm the loading of the lysine on mesoporous materials, back titration was performed (Table 1). It is found that

SBA-15-COOH gives a loading of 0.622 mmol/g of $-COOH$. However, Pro-proximal-C-A-SBA-15 and Pro-maximum-C-A-SBA-15 give small amount of loading of -COOH, indicating that almost all carboxyl groups were reacted with amino groups of lysine. In addition, it is found that proximal-C-A-SBA-15 gives a loading of 0.613 mmol/g of $-COOH$ and maximum-C-A-SBA-15 gives a loading of 0.615 mmol/g of $-COOH$, which are in good agreement with the loading of $-NH_2$ obtained by elemental analysis results.
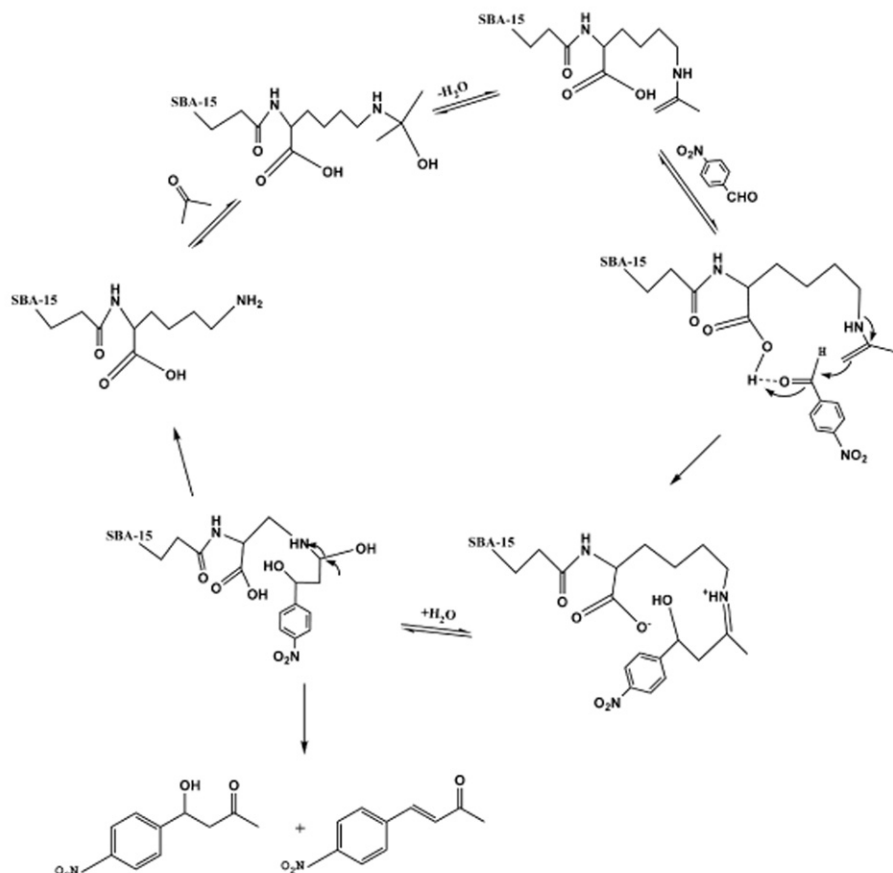
Table 2
Test of catalysts. Catalysis data

Entry	R	Catalyst[a]	A%	B%	Total conversion[b]	TON[c]
1	NO$_2$	Carboxyl-SBA-15	–	–	Trace	–
2	NO$_2$	L-lysine/SBA-15[d]	52	8	60	–
3	NO$_2$	Pro-proximal-C-A-SBA-15	–	–	Trace	–
4	NO$_2$	Pro-maximum-C-A-SBA-15	–	–	Trace	–
5	NO$_2$	Proximal-C-A-SBA-15	71	19	90	7.4
6	NO$_2$	Maximum-C-A-SBA-15	57	17	74	6
7	CF$_3$	Proximal-C-A-SBA-15	54	28	82	6.7
8	CF$_3$	Maximum-C-A-SBA-15	38	27	65	5.3
9	CN	Proximal-C-A-SBA-15	62	24	86	7
10	CN	Maximum-C-A-SBA-15	49	12	61	5

[a] 0.5 mmol 4-nitrobenzaldehyde in 10 ml acetone stirred at 50 °C for 20 h.
[b] Conversion calculated by ^{1}H NMR spectroscopy analysis.
[c] Number of moles of aldehyde converted per 1 mol of –COOH.
[d] Physical mixture of L-lysine and SBA-15.

Scheme 2. Proposed reaction mechanism for the aldol condensation reaction on the solid support.

3.2. Catalytic test

The catalytic properties of synthetic materials are shown in Table 2. The carboxyl-SBA-15, Pro-proximal-C-A-SBA-15, and Pro-maximum-C-A-SBA-15 almost gave no conversion (entries 1, 3, and 4). However, after deprotection, proximal-C-A-SBA-15 and maximum-C-A-SBA-15 gave higher level conversion. Compared with lysine/SBA-15, maximum-C-A-SBA-15 (entry 6) gave rise to 74% conversion of 4-nitrobenzaldehyde. When using proximal-C-A-SBA-15 as catalyst (entry 5), 90% conversion of 4-nitrobenzaldehyd was achieved. Also, proximal-C-A-SBA-15 showed a higher TON value than maximum-C-A-SBA-15, indicating that the rate of per site was enhanced by proximal-C-A-SBA-15. In addition, the catalytic properties of synthetic materials have also been tested in aldol condensation reaction between acetone and other aldehydes with electron-withdrawing group (entries 7–10), and proximal-C-A-SBA-15 still exhibited higher conversion and TON value than maximum-C-A-SBA-15.

Compared to maximum-C-A-SBA-15, proximal-C-A-SBA-15 was more active toward aldol condensation while containing almost the same amount of lysine. These results indicate that the acid–base cooperation effect should be involved in the catalytic reaction. The probable cooperative mechanism is shown in Scheme 2. Dual activation of electrophiles and nucleophiles at the acidic sites and the basic sites is elaborated. The aldehyde gets activated by the acidic sites, and acetone is deprotonated to generate imine formation by the basic sites, which then attacks the electron-deficient aldehyde to generate the aldol product. We can adjust acid–base distance within a certain range to prevent the mutually destructive between acidic site and basic site. However, the activity decreased as the acid–base distance growed. It indicates that cooperative surface catalysis relies on the two functional groups being close enough to each other on the surface to interact with each other or with the reacting molecules. Also, maximum acid–base distance is not conducive to protonated transmission.

4. Conclusions

In conclusion, a novel method for successful synthesis of acid–base bifunctional heterogeneous catalysts by immobilizing the lysine on mesoporous solid was described. XRD, TEM, and N_2 adsorption–desorption provided evidence that the functionalized materials kept mesostructure. FTIR, TGA, elemental analysis, and back titration confirmed that the lysine was successfully incorporated into the mesoporous SBA-15. Compared with maximum-C-A-SBA-15, proximal-C-A-SBA-15 displayed excellent catalytic activity and TON value in the aldol condensation reaction. It indicates that cooperative surface catalysis relies on the two functional groups being close enough to each other on the solid surface to interact with each other or with the reacting molecules.

Acknowledgments

References

[1] I. Rodriguez, S. Iborra, A. Corma, F. Rey, J.L. Jordá, Chem. Commun. (1999) 593–594.
[2] A. Stein, Adv. Mater. 15 (2003) 763–775.
[3] I.K. Mbaraka, D.R. Radu, V.S.Y. Lin, B.H. Shanks, J. Catal. 219 (2003) 329–336.
[4] X.G. Wang, C.C. Chen, S.Y. Chen, Y. Mou, S. Cheng, Appl. Catal. A: Gen. 281 (2005) 47–54.
[5] V.S.Y. Lin, C.Y. Lai, J. Huang, S.A. Song, S. Xu, J. Am. Chem. Soc. 123 (2001) 11510–11511.
[6] S. Dai, M.C. Burleigh, Y. Shin, C.C. Morrow, C.E. Barnes, Z. Xue, Angew. Chem. Int. Ed. 38 (1999) 1235–1239.
[7] H. Hata, S. Saeki, T. Kimura, Y. Sugahara, K. Kuroda, Chem. Mater. 11 (1999) 1110–1119.
[8] W. Zhou, J.M. Thomas, D.S. Shephard, B.F.G. Johnson, D. Ozkaya, T. Maschmeyer, R.G. Bell, Q. Ge, Science 280 (1998) 705–708.
[9] W.H. Zhang, X.B. Lu, J.H. Xiu, Z.L. Hua, L.X. Zhang, M. Robertson, J.L. Shi, D.S. Yan, J.D. Holmes, Adv. Funct. Mater. 14 (2004) 544–552.
[10] X.G. Wang, Y.H. Tseng., J.C.C. Tseng, S. Cheng, Microporous Mesoporous Mater. 85 (2005) 241–251.
[11] A.S.M. Chong, X.S. Zhao, J. Phys. Chem. B 107 (2003) 12650–12657.
[12] J.A. Melero, G.D. Stucky, R.V. Grieken, G. Morales, J. Mater. Chem. 12 (2002) 1664–1670.
[13] E.C. Serrano, J.M.C. Martin, J.L.G. Fierro, Chem. Commun. 14 (2003) 246–247.
[14] M.G. Cazalilla, J.M.M. Robles, A. Gurbani, E.R. Castellona, A.J. Lopez, J. Solid State Chem. 180 (2007) 1130–1140.
[15] C.M. Yang, B. Zibrowius, F. Schüth, Chem. Commun. 14 (2003) 1772–1773.
[16] J.D. Bass, A. Solovyov, A.J. Pascall, A. Katz, J. Am. Chem. Soc. 128 (2006) 3737–3747.
[17] F. Gelman, J. Blum, D. Avnir, Angew. Chem. Int. Ed. 40 (2001) 3647–3649.
[18] S. Shylesh, A. Wagner, A. Seifert, S. Ernst, W.R. Thiel, Chem. Eur. J. 15 (2009) 7052–7062.
[19] R.K. Zeidan, V. Dufaud, M.E. Davis, J. Catal. 239 (2006) 299–306.
[20] R.K. Zeidan, M.E. Davis, J. Catal. 247 (2007) 379–382.
[21] R.K. Zeidan, S.J. Hwang, M.E. Davis, Angew. Chem. Int. Ed. 45 (2006) 6332–6335.
[22] H. Li, X.B. Lu, Chin. J. Catal. 30 (2009) 587–589.
[23] S. Shylesh, A. Wagner, A. Seifert, S. Ernst, W.R. Thiel, Chem. Eur. J. 15 (2009) 7052–7062.
[24] S. Huh, H.T. Chen, J.W. Wiench, M. Pruski, V.S.Y. Lin, Angew. Chem. Int. Ed. 44 (2005) 1826–1830.
[25] D. Srinivas, P. Ratnasamy, Microporous Mesoporous Mater. 105 (2007) 170–180.
[26] Y.Q. Shao, J.Q. Guan, S.J. Wu, H. Liu, B. Liu, Q.B. Kan, Microporous Mesoporous Mater. 128 (2010) 120–125.
[27] J. Alauzun, A. Mehdi, C. Reye, J.P. Corriu, J. Am. Chem. Soc. 128 (2006) 8718–8719.
[28] H. Li, S.T. Xu, W.P. Zhang, X.B. Lu, Chin. Chem. Lett. 20 (2009) 1051–1054.
[29] E.L. Margelefsky, A. Bendjériou, R.K. Zeidan, V. Dufaud, M.E. Davis, J. Am. Chem. Soc. 130 (2008) 13442–13449.
[30] E.L. Margelefsky, R.K. Zeidan, V. Dufaud, M.E. Davis, J. Am. Chem. Soc. 129 (2007) 13691–13697.
[31] J.D. Bass, A. Katz, Chem. Mater. 18 (2006) 1611–1620.
[32] S.L. Hruby, B.H. Shanks, J. Catal. 263 (2009) 181–188.
[33] E. Angeletti, C. Canepa, G. Martinetti, P. Venturello, J. Chem. Soc. Perkin Trans. 1 (1989) 105–107.
[34] B. List, R.A. Lerner, C.F. Barbas III, J. Am. Chem. Soc. 122 (2000) 2395–2396.
[35] E.G. Doyaguez, F. Calderón, F. Sánchez, A.F. Mayoralas, J. Org. Chem. 72 (2007) 9353–9356.
[36] G. Yang, Z.W. Yang, L.J. Zhou, R.X. Zhua, C.B. Liu, J. Mol. Catal. A: Chem. 316 (2010) 112–117.
[37] A. Córdova, W.B. Zou, I. Ibrahem, E. Reyes, M. Engqvist, W.W. Liao, Chem. Commun. 28 (2005) 3586–3588.
[38] J.M. Oh, S.J. Choi, G.E. Lee, S.H. Han, J.H. Choy, Adv. Funct. Mater. 19 (2009) 1617–1624.
[39] M. Luechinger, A. Kienhöfer, G.D. Pirngruber, Chem. Mater. 18 (2006) 1330–1336.